

Evolution of *Protoanancus* (Proboscidea, Mammalia) in East
Asia

SHIQI WANG,^{*,1} TAO DENG,¹ TAO TANG,¹ GUANGPU XIE,² YUGUANG
ZHANG,³ and DUOQING WANG⁴

¹Key Laboratory of Evolutionary Systematics of Vertebrates, Institute of Vertebrate
Paleontology and Paleoanthropology, Chinese Academy of Sciences, Beijing 100044,
China, wangshiqi@ivpp.ac.cn;

²Gansu Provincial Museum, Lanzhou, Gansu Province 730050, China;

³Beijing Natural History Museum, Beijing 100050, China;

⁴Qin'an Museum, Qin'an, Gansu Province 741600, China

Journal of Vertebrate Paleontology, Volume 35, 2015

*Corresponding author.

DESCRIPTIONS OF THE SPECIMENS

Protanancus tobieni

BPV-261—is a palate and a pair of hemimandibles from the same individual (Figs. 2A, 2B, 2G, and 2H, also see Guan, 1988:pl. I [1–4], 1996:figs. 13.2a, b, f, g). However, the mandibular symphysis is broken. The palate carries left P4, fully worn left and right M1s, moderately worn M2s, and newly erupted M3s. P4 is oval with two lophs and an anterior and a posterior cingulum. The pretrite half-lophs are trifoliate and each posttrite half-loph shows a main cusp and a mesoconelet. The M1 and M2 are trilophodont, and M1 is fully worn. On the M2, the trefoils are well expressed on the first two pretrite half-lophs, but the posterior accessory central conule is absent on the third pretrite half-loph. Posttrite ornamentation is present on the first two lophs. The M3 is recently erupted and exhibits first and partial second lophs. The first pretrite half-loph is trifoliate and the posttrite half-loph has only a main cusp and mesoconelet. The hemimandibles carry a moderately worn left m2 and partially erupted left and right m3s (the right m2 may have been shed or broken). The m2 is trilophodont with a posterior cingulid. The pretrite trefoils are well developed and a prominent anterior posttrite accessory central conule is seen on the third lophid. The cingulid is composed of two enamel cusps, of which the pretrite one is more prominent. The first three lophids are seen in the just-erupted m3. Trefoils are developed on the first two pretrite half-lophids, and ornamentation is present on the first posttrite half-lophid. However, on both the pretrite and posttrite sides of the third lophid, the anterior accessory central conules are prominent but posterior accessory central conules are absent. The pretrite and posttrite half-lophids occupy somewhat alternating positions (pseudo-anancoidy), although this feature is fairly weak. A relatively small amount of cementum is present in the interlophids of the cheek teeth.

BPV-670—is a palate with deeply worn M2s and moderately worn M3s (Fig. 2C and 2I, also see Guan, 1988:pl. II [2], 1996:figs. 13.4a, b). It was originally referred to as '*Serbelodon zhongningensis*' by Guan (1988). The basic crown structure is similar to that of BPV-261. Although deeply worn, posttrite ornamentation is present on the M2. The M3 has four lophs. The first two pretrite half-lophs are trifoliate and the third pretrite half-loph has only an anterior accessory central conule. Posttrite ornamentation on the posterior half-lophs is either weak or absent. The fourth loph is composed of a row of enameled cusps. The cementum in the interlophs is weak.

BPV-590—is a complete right lower incisor (Figs. 2D and 2E, also see Guan, 1988:pl. I [3], 1996:figs. 13.2d, e). The tusk is flattened, long and narrow, concave upward from the lateral view, and slightly clockwise twisted in anterior view. The anteromedian angle is quadrate and the anterolateral angle is rounded. The cross section is biconcave with the dorsal surface more concave than the ventral one.

BPV-1555—comprises a left and a right upper incisor (Fig. 2F, also see Guan, 1988:pl. I [2]). The incisors are curved with wide enamel bands on the lateral sides; the curvature is not significant relative to that seen in *Protanancus macinnesi* (Tassy, 1986). However, these incisors may be ontogenetically young.

QA1248-45—is a complete mandible with deeply worn m3s (Figs. 3A, 3B and

3G). The mandibular symphysis is trough-shaped and elongated, but it is not as long as that in the type specimens *Protanancus chinjiensis* and *Amebelodon fricki* (Barbour, 1927, 1929a; Osborn, 1929) and the distal edge is obscured by plaster reconstruction. The maximum width of the symphysis is slightly posterior to the distal edge; the narrowest position is at the proximal end of the mandibular symphysis. There is no transverse ledge at the narrowest part of the symphysis as occurs in *Platybelodon grangeri*. The ramus is thin and tilts posteriorly by an angle of 128° with respect to the corpus, showing a shallow masseteric fossa and a rounded angular process. The mandibular condyle is a transversely oriented cylindrical bar. The m3 (Fig. 3G) has five lophids, with the first two worn out completely. The trefoils are developed on the third and fourth pretrite half lophids; posttrite ornamentation is present. The fifth lophid is composed of two enameled cusps of which the pretrite is more prominent. The pseudo-ananoid contacts of the half lophids and the cementum are weak.

QA1256-46—is a complete left upper incisor (Figs. 3C and 3D), which probably belongs to the same individual as QA1248-45 based on the accounts of the excavators. The incisor is strong, with an enamel band on its ventro-lateral surface. A wear surface adjacent to the enamel band is present on the ventral surface. A sharp edge between the wear surface and the enamel band is formed. The enamel band is 44.5 mm thick at the anterior part, but narrows and eventually vanishes at the posterior part of the incisor. The oval cross-section shows ~10 internal laminae.

IVPP V 2407, QA0979-0030, and QA0951-002— (Figs. 3E and 3F, also see Zhai, 1959:pl. 1 [figs. 1, 1A]; Tobien et. al, 1986:fig. 24) are fragmentary anterior parts of i2. The widths and heights of these teeth are variable (Table 1), suggesting their different ontogenetic stages. However, all of the cross-sections are biconcave, with 10–15 internal laminae.

Protanancus brevirostris

IVPP V 17687—represents a very old individual with fully worn cheek teeth (Figs. 4A–C, 5A–F, 5I, and 5J). The cranium and mandible are largely deformed and many irregular cavities are present on the surface of the specimen, probably caused by serious osteoporosis. The left zygomatic arch and the occipital part are broken. Cranium (Figs. 4A and 4B): In the dorsal view, the incisive alveolus is long and slender. It tapers at its anterior part with a narrow incisive fossa between the two alveoli. The upper incisors are absent. The temporal lines converge at the dorsal part of the neurocranium. The squamosal bone is laterally expanded, connecting with the slender jugal. In the ventral view, the palate between the tooth rows is narrow. The transversely elongated infraorbital foramen is located at the ventral side of the anterior edge of the zygomatic process. The posterior nasal aperture is oval with a thin vomer present in the middle. The front edge of the posterior nasal aperture is posterior to the posterior end of M3. The basioccipital and basisphenoid bones are tightly fused. The occipital condyles are broken around a dorso-ventrally compressed foramen magnum. Most of the tympanic bulla and glenoid region are poorly preserved. In the lateral view, most of the structures are damaged by dorso-ventral compression, although the anterior border of the orbit is in line with the posterior part of the M3, evidencing a

relatively developed face. The tetra-lophed M3 is fully worn, whereas the tri-lophed M2 is still preserved (Fig. 5I).

Mandible (Fig. 4C): The mandibular symphysis is elongated, but shorter than that of *Protanancus tobieni*. The maximal width of the symphysis is at its distal end, with its narrowest position located at its proximal root, without a transverse ledge at the narrowest part of the symphysis. The anterior edge of the incisive alveolus is oblique anteriorly towards the median axis, forming an angle with the apex oriented anteriorly between the two alveoli. The corpus is prominent, with two mental foramina, of which the posterior one is large and rounded beneath the m2 and the anterior one is slit-like and located 80 mm in front of the posterior one. The ramus is thin and tilts posteriorly at an angle of 125° with the corpus, with a shallow masseteric fossa. The coronoid process is rounded and directed dorsally, while the mandibular condyle is transversely oriented. As in the skull, the tri-lophided right m2 is still preserved even though the tetra-lophided m3s are fully worn; the left m2 was either shed or it broke.

i2 (Figs. 5A–F): The right i2 was probably shed before death and the remaining left i2 is long (Fig. 5A). The cross-section at the anterior edge of the right alveolus is greatly flattened (perhaps because of over-use), with a thin layer of dentine wall enclosing a hollow cavity (Fig. 5E). However, it is biconcave at its more anterior part (Figs. 5B–D). There is a wear facet on the dorsal side of the anterior end (about 250 mm anterior to the anterior edge of alveolus), that bears a concentric laminar structure, seen in anterior view (Fig. 5F).

HMV1782–1, 2, 3—are three anterior fragments of DI2 (Fig. 5G). DI2 is slender and the tip is blunt, with a thick lateral enamel band.

HMV1873—is a left dentary with a deeply worn m2 and unworn m3 (Fig. 5H). The m2 has pretrite trefoils and anterior posttrite accessory central conules (posttrite ornamentation) of the second and third lophids. The posterior cingulid is even weaker than the m2 of *Pr. tobieni*. The m3 has strong pretrite trefoils and weak posttrite ornamentation on the first two lophids. On the third lophid of m3, the pretrite anterior accessory central conule and the mesoconelet are fused with a diminished posterior accessory central conule, but the posttrite anterior accessory central conule is prominent. The fourth lophid is composed of a row of enameled cusps. However, pseudo-anancoidy is even weaker than that in *Pr. tobieni*.

LITERATURE CITED

- Barbour, E. H. 1927. Preliminary notice of a new proboscidean *Amebelodon fricki*, gen. et sp. nov. Bulletin of the Nebraska State Museum 13:131–134.
- Barbour, E. H. 1929a. The mandible of *Amebelodon fricki*. Bulletin of the Nebraska State Museum 15:139–146.
- Barbour, E. H. 1929b. The mandibular tusks of *Amebelodon fricki*. Bulletin of the Nebraska State Museum 14:135–138.
- Barbour, E. H. 1929c. *Torynobelodon loomisi*, gen. et sp. nov. Bulletin of the Nebraska State Museum 16:147–153.

- Frick, C. 1933. New remains of trilophodont-tetrabelodont mastodons. *Bulletin of the American Museum of Natural History* 56: 505–652.
- Gaziry, A. W. 1976. Jungtertiäre Mastodonten aus Anatolien (Türkei). *Geologisches Jahrbuch* B22:3–143.
- Guan, J. 1988. The Miocene strata and mammals from Tongxin, Ningxia and Guanghe, Gansu. *Memoirs of Beijing Natural History Museum* 42:1–21. [Chinese 1–19; English 20–21]
- Guan, J. 1996. On the shovel-tusked elephantoids from China; pp. 124–135 in J. Shoshani and P. Tassy, (eds.), *The Proboscidea: Evolution and Palaeoecology of Elephants and Their Relatives*. Oxford University Press, Oxford.
- Lambert, W. D. 1990. Rediagnosis of the genus *Amebelodon* (Mammalia, Proboscidea, Gomphotheriidae), with a new subgenus and species, *Amebelodon (Konobelodon) britti*. *Journal of Paleontology* 64:1032–1040.
- Markov, G. N., and S. Vergiev. 2010. First report of cf. *Protanancus* (Mammalia, Proboscidea, Amebelodontidae) from Europe. *Geodiversitas* 32:493–500.
- Osborn, H. F. 1929. New Eurasiatic and American proboscideans. *American Museum Novitates* 393:1–28.
- Osborn, H. F. 1936. *Proboscidea: a monograph of the discovery, evolution, migration and extinction of the mastodons and elephants of the world*. The American Museum Press, New York, 802 pp.
- Pickford, M. 2003. New Proboscidea from the Miocene strata in the lower Orange River Vally, Namibia. *Memoir Geological Survey Namibia* 19:207–256.
- Tassy, P. 1986. Nouveaux Elephantoidea (Proboscidea, Mammalia) dans le Miocène du Kenya: essai de réévaluation systématique. *Cahiers de Paléontologie*. E'ditions du Centre National de la Recherche Scientifique, Paris, 135 pp.
- Tassy, P. 1983. Les Elephantoidea Miocènes du Plateau du Potwar, Groups de Siwalik, Pakistan. I^{re} Partie: Cadre chronologique et géographique, Mammutidés, Amébélodontidés. *Annales de Paléontologie* 69:99–136.
- Tassy, P. 1996. Growth and sexual dimorphism among Miocene elephantoids: the example of *Gomphotherium angustidens*; pp. 92–100 in J. Shoshani and P. Tassy, (eds.), *The Proboscidea: Evolution and Palaeoecology of Elephants and Their Relatives*. Oxford University Press, Oxford.
- Tobien, H. 1973. On the evolution of Mastodonts (Proboscidea, Mammalia). Part 1: the bunodont trilophodont groups. *Notizblatt des Hessischen Landesamtes für Bodenforschung zu Wiesbaden* 10:202–276.
- Tobien, H., G.-F. Chen, and Y.-Q. Li. 1986. Mastodonts (Proboscidea, Mammalia) from the late Neogene and early Pleistocene of the People's Republic of China. Part I: Historical account: the genera *Gomphotherium*, *Choerolophodon*, *Synconolophus*, *Amebelodon*, *Platybelodon*, *Sinomastodon*. *Mainzer Geowissenschaftliche Mitteilungen* 15:119–181.
- Wang, B.-Y., and Z.-X. Qiu. 2002. A new species of *Platybelodon* (Gomphotheriidae, Proboscidea, Mammalia) from early Miocene of the Danghe area, Gansu, China. *Vertebrata Palasiatica* 40:291–299. [Chinese 291–296; English 297–299]

- Wang, S.-Q., W. He, and S.-Q. Chen. 2013. Gomphotheriid mammal *Platybelodon* from the middle Miocene of Linxia Basin, Gansu, China. *Acta Palaeontologica Polonica* 58: 221–240.
- Zhai, R.-J. 1959. [Discovery of some Miocene mammals from Ching-an, eastern Kansu]. *Vertebrata Palasiatica* 1:139–140. [Chinese]

SUPPLEMENTARY TABLES

TABLE S1. Mandibular measurements (in mm, follow Tassy, 1996, slightly revised) from *Protanancus tobieni* (QA 1248–45) and *Pr. brevirostris* sp. nov. (IVPP V17687).

Specimens No.	QA 1248 –45	IVPP V 17687
maximum length (1)	1406	1153
symphyseal length (2)	530	299
alveolar distance (from the most salient point of the trigonum retromolare to the symphyseal border of the corpus) (3)	ca 426	316
ventral length measured from the gonion (angulus mandibular) to the tip of the symphysis (4)	1012	660
maximum width (5)	229 × 2	–
mandibular width measured at the root of the rami (6)	337	–
width of corpus measured at the root of the ramus (7)	112	70
width of corpus measured at the anterioralveolus (or the grinding tooth if the alveolus is entirely resorbed) (8)	55	48
posterior symphyseal width (9)	166	154
anterior symphyseal width (10)	238	204
maximum symphyseal width (11)	242	204
minimum symphyseal width (12)	131	134
maximum width of rostral trough (13)	194	160
minimum width of rostral trough (14)	66	47
internal width between anterior alveoli (or grinding teeth if the alveoli are resorbed) (15)	64	57
maximum height of corpus (measurement taken perpendicular to the ventral border of the corpus) (16)	160	91
height of corpus measured at the root of the ramus (measurement as above) (17)	122	105
rostral height measured at the symphyseal border (measurement taken perpendicular to the ventral border of the symphyseal rostrum) (18)	135	52
rostral height measured at the tip of rostrum (measurement as above) (19)	61	25
maximum mandibular height measured at the condyle perpendicular to the ventral border of the corpus (20)	291	215
maximum depth of ramus (21)	205	185
depth between gonion and coronoid processes (22)	206	–
height between gonion and condyle (23)	273	–
mid-alveolar length measured on the buccal side between the anterior alveolus (or grinding tooth if the alveolus is resorbed) and the root of the ramus (24)	303	197

TABLE S2. Cranial measurements (in mm, follow Tassy, 1996, slightly revised) from *Protanancus brevirostris* sp. nov. (IVPP V17687).

maximal length measured from the occipital border (1)	765
length of cerebral part (2)	300
length of premaxilla (3)	403
length of incisive fossa (4)	371
length of nasal bones from the tip to the upper border of the nasal fossa (5)	25
maximal supraorbital width (6)	462
posterior rostral width (as measured between the infraorbital foramina) (7)	240
anterior rostral width (8)	157
width of nasal bones at the upper border of the nasal fossa (9)	80
width of nasal fossa (10)	246
minimal cerebral width between temporal lines (11)	84
maximal length measured from the condyles (12)	730
length of zygomatic arch measured from the processus zygomaticus of the maxilla to the posterior border of the glenoid fossa (13)	400
length of orbitotemporal fossa measured at the level of the zygomatic arch (14)	218
palatal length from the anterior grinding tooth to the choanae (15)	270
length of basicranium from the choanae to the foramen magnum (16)	258
thickness of processus zygomaticus of the maxilla (17)	133
maximal cranial width across the zygomatic arches (18)	450
width of basicranium between the lateral borders of the glenoid fossae (19)	355
maximal width of choanae (20)	50
internal maximal width of the palate (21)	90
external maximal width of the palate (22)	198
internal width of the palate measured at the anterior grinding teeth (23)	45
minimal palatal width between the inter-alveolar cristae (maxillary ridges) (24)	81
sagittal height of occipital (25)	–
occipital width (26)	360
height of premaxilla (27)	–
facial height measured at the anterior grinding tooth (28)	–
height of the maxilla ventral to the processus zygomaticus (29)	–
height of the orbit (30)	–
cranial height measured from the top of the cranium to the pterygoid process (31)	–
length of basicranium from the condyles to the pterygoid process (32)	265
facial length measured from the tip of the rostrum to the pterygoid process (33)	465
length of the orbitotemporal fossa measured from the squamosal to the anterior border of the orbit (34)	255
mid-cranial length measured from the external auditory meatus to the ventral border of the orbit (35)	325
mid-cranial height measured from the pterygoid process to the dorsal border of the orbit (36)	–

TABLE S3. Material examined in the microwear analyses.

Species	Specimen No.	Loc.	Tooth position	Loph(id) examined	Scratches	Pits	
<i>Protanancus tobieni</i>	BPV261	Dingjiaergou, Tongxin	l. M2	1	102	8	
			r. M2	1	103	8	
			l. m2	2	94	11	
			l. m3	1	83	18	
			r. m3	1	70	9	
	BPV670		l. M3	1	80	20	
			l. M2	2	85	5	
	BPV000906		r. M1	1	88	5	
	<i>Platybelodon danovi</i>	IVPP V5572	Dingjiaergou, Tongxin	l. m3	2	91	7
				l. M3	2	83	16
r. m3				2	105	7	
IVPP V8030			l. m3	2	94	6	
			r. m2	1	92	6	
			r. m3	2	92	7	
			r. m3	2	106	5	
IVPP V8037			l. m2	1	76	4	
IVPP V8039			l. m2	1	85	6	
IVPP V8044			l. m1	2	94	6	
<i>Platybelodon grangeri</i>	HMV0019	Zengjia,	l. M3	1	107	10	
	HMV0029	Linxia	l. m3	2	77	9	
	HMV0041		l. m2	1	82	19	
	HMV0042		l. M3	1	79	13	
	HMV0044		r. m1	1	52	20	
	HMV0828		r. m2	1	79	11	
	HMV0940		l. M3	2	81	8	
	HMV1828		l. M2	2	105	24	

TABLE S4. Results of the t-tests following microwear analyses. The black font denotes significant difference (at the significant level $\alpha = 0.05$)

P-values	<i>Pr. tobieni</i>	<i>Pl. danovi</i>	<i>Pl. grangeri</i>	
<i>Pr. tobieni</i>		0.1185	0.2162	Numbers of pits
<i>Pl. danovi</i>	0.4551		0.0046	
<i>Pl. grangeri</i>	0.4728	0.1723		
	Numbers of scratches			

SUPPLEMENTARY FIGURE CAPTIONS

FIGURE S1. Maps showing fossil localities of the specimens discussed in the present article. **A**, localities of the Amebelodontinae fossils in East Asia; **B**, localities of *Protanancus* fossils. **Abbreviations:** **EM**, early Miocene, **MM**, middle Miocene, **Pb**, *Protanancus brevirostris* sp. nov., **Pdh**, *Platybelodon dangheensis*, **Pdv**, *Pl. danovi*, **Pg**, *Pl. grangeri*, **Pt**, *Pr. tobieni*.

FIGURE S2. Microwear analyses of *Protanancus tobieni*, *Platybelodon danovi*, and *Platybelodon grangeri*. **A**, occlusal view of right M2 of BPV261 shows the shearing facets examined; **B**, digitized photographs of the shearing facets; **C**, histogram showing the statistics of the numbers of scratches and pits determined for the three species. Bars represent means; errors represent standard deviations. The asterisk indicates significant difference ($\alpha = 0.05$).

FIGURE S3. Bivariate plots of amebelodontine teeth and mandibular measurements.

SUPPLEMENTARY FIGURES

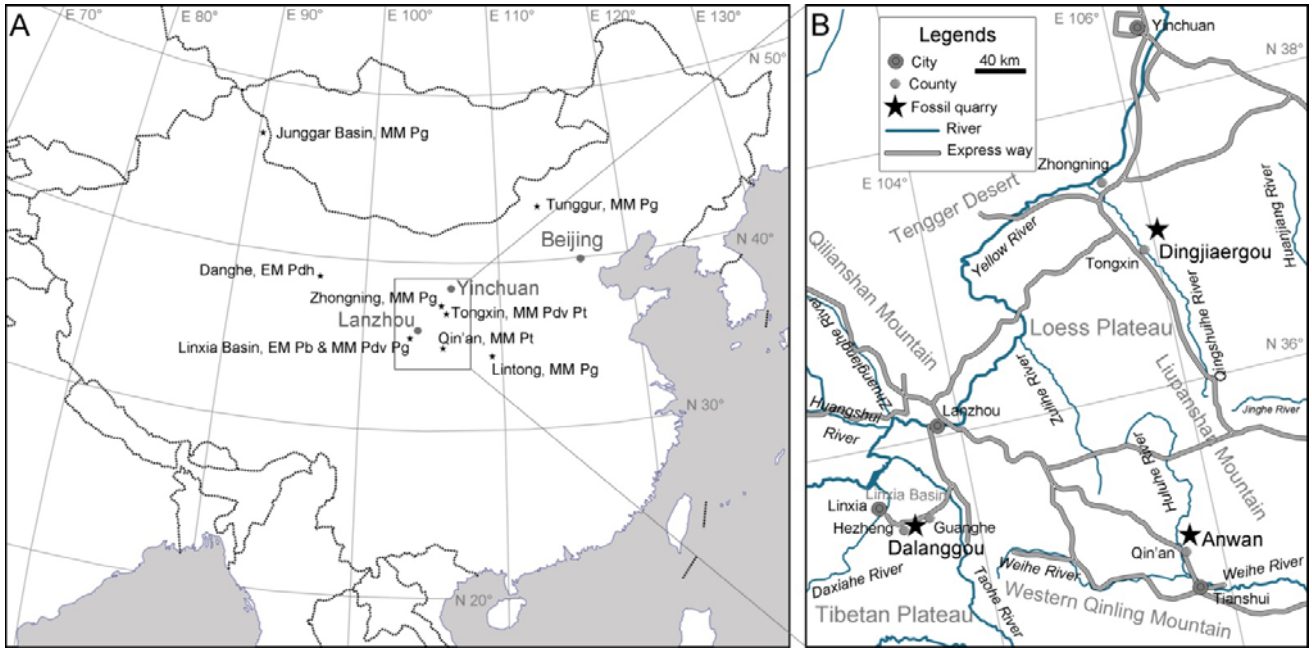


Figure S1

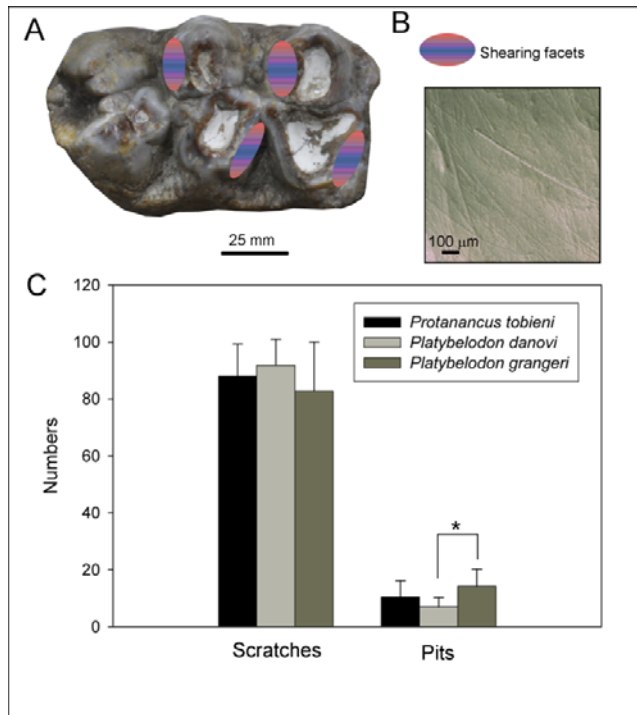
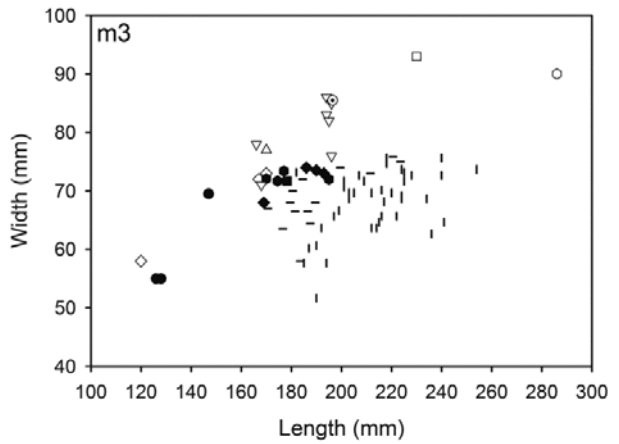
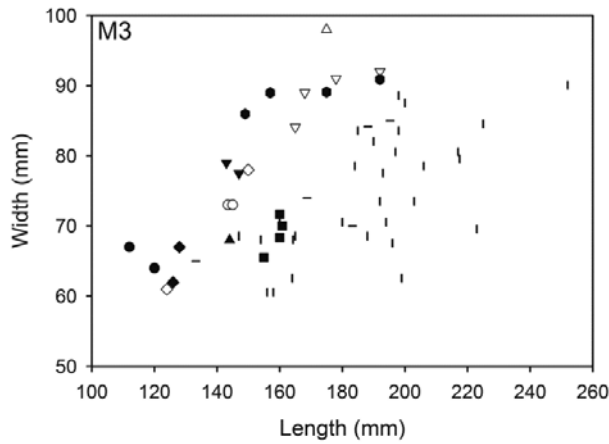
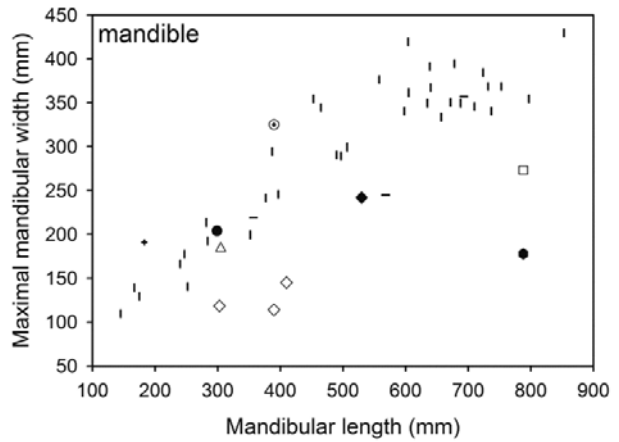
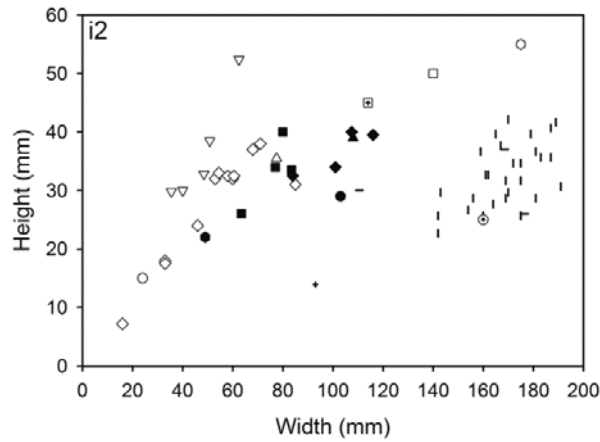


Figure S2



- *cf. Archaeobelodon*, data from Tassy, 1986
- ◇ *Archaeobelodon filholi*, data from Tobien, 1973
- △ *Serbelodon barbourensis*, data from Frick, 1933
- ▽ *Afromastodon coppensi*, data from Pickford, 2003
- *Protanancus breviostris* sp. nov.
- ◆ *Protanancus tobieni*
- *Protanancus macinnesi*, data from Tassy, 1986
- *Protanancus chinjiensis*, data from Tassy, 1983

- ▲ *Protanancus* sp. (Yürükali), data from Gaziry, 1976
- ▼ *cf. Protanancus* (Vetren), data from Markov and Vergiev, 2010
- *Amebelodon fricki*, data from Babour, 1929a, b
- *Amebelodon britti*, data from Lambert, 1990
- *Platybelodon dangheensis*, data from Wang and Qiu, 2002
- *Platybelodon danovi*, data from Wang et al., 2013
- ! *Platybelodon grangeri*, data from Wang et al., 2013
- ⊙ *Torynobelodon barnumbrowni*, data from Osborn, 1936
- ▣ *Torynobelodon loomisi*, data from Barbour, 1929c

Figure S3